Phase Diagram in the Kicked Harper Model

R. Artuso,[1,2] F. Borgonovi,[3,4] I. Guarneri,[4,5] L. Rebuzzini,[3] and G. Casati[2,5]
[1]*Dipartimento di Fisica, Università di Milano, Via Celoria 16, 20133 Milano, Italy*
[2]*Istituto Nazionale di Fisica Nucleare, Sezione di Milano, Via Celoria 16, 20133 Milano, Italy*
[3]*Dipartimento di Fisica Nucleare e Teorica, Università di Pavia, Via Bassi 6, 27100 Pavia, Italy*
[4]*Istituto Nazionale di Fisica Nucleare, Sezione di Pavia, Via Bassi 6, 27100 Pavia, Italy*
[5]*Università di Milano, Sede di Como, Via Castelnuovo 7, 22100 Como, Italy*
(Received 6 July 1992)

The kicked Harper model is numerically investigated. The long-time nature of the wave function dynamics and a multifractal analysis of the spectrum provide evidence for the existence of different regimes marked by different spectral types and diffusion exponents, with a phase diagram substantially different from that of the standard Harper model.

PACS numbers: 05.45.+b, 03.65.−w, 73.20.Dx

A thorough understanding of quantum dynamics of systems with chaotic classical analogs represents a theoretical challenge of considerable interest. A number of remarkable results have been derived in the last few years, concerning features like eigenvalue statistics and the emerging role of classical unstable orbits as an invisible skeleton underlying the organization of quantum motion (see [1,2], to which we also refer for original references). In particular, the investigation of the quantum behavior of classically diffusive systems has unveiled the phenomenon of dynamical localization, thus bringing into light an interesting parallel with the quantum dynamics in disordered or incommensurate structures. This parallel is especially close in a recently introduced model [3], known as the kicked Harper (KH) model, which is also the subject of the present paper. Under appropriate conditions, this model exhibits some sort of diffusion in both the classical and the quantum cases (the connection between classical and quantum diffusion is unclear though). This marks an important difference from most previously studied one-dimensional, periodically driven models, where diffusion is totally quenched by quantum localization [4], and also with the standard Harper model which exhibits diffusion [5] but has an integrable classical limit.

The KH model is obtained upon quantization of the Harper map

$$p_{n+1}=p_n+K\sin(x_n),\quad x_{n+1}=x_n-L\sin(p_{n+1})\ (\mathrm{mod}2\pi)\,. \tag{1}$$

This map (which can be considered as a discrete-time version of the classical Harper model [6]) has been considered as a model of an electron in perpendicular magnetic and electric fields, and has also been related to the problem of stochastic heating of plasma in a magnetic field (see [7]). The corresponding quantum system has been the object of many recent studies: It displays the same type of duality that characterizes the Harper model [8] and this gives strong mathematical support for the existence of extended quasienergy eigenstates in some region of the (K,L) plane [9]. As a matter of fact, earlier references [10–12] suggested that quantum behavior is quite akin to that of the Harper model, being characterized by the same kind of localized-extended-state transition [13]. Further analysis signaled dynamical anomalies [14], and revealed a complex structure of the critical $(K=L)$ line, leading to anomalous diffusion and nontrivial multifractal properties of the spectrum [15]. Our aim is to characterize the phase diagram of this model, and to show how it differs dramatically from the Harper case, being characterized by a transition from localization to unbounded spreading in the subcritical $(K<L)$ region.

Quantization of the map (1) leads to the one-period evolution operator

$$\mathbf{U}_{L,K}=\exp\left(-i\frac{L}{\hbar}\cos(\hbar\hat{n})\right)\exp\left(-i\frac{K}{\hbar}\cos(x)\right),$$

where $\hat{n}=-i\partial/\partial x$. Quasienergy eigenvalues and eigenvectors are determined by $\mathbf{U}_{L,K}\psi_\omega=e^{-i\omega}\psi_\omega$. We will investigate the incommensurate case, with $\hbar/2\pi$ given by a quadratic irrational [our examples will concern the case $\hbar=2\pi/(6+\rho_{\mathrm{GM}})$, $\rho_{\mathrm{GM}}=(1+\sqrt{5})/2$]. The "unit-time" propagator of the standard Harper model is recovered via the limit $\lim_{t\to\infty}\mathbf{U}_{Lt^{-1},Kt^{-1}}^{t}$. We recall that for the Harper model (i.e., if the potential is not time modulated by the δ function), for $K<L$ we get localization, while for $K>L$ all the states are extended (leading to ballistic propagation); for $K=L$ we have critical states [13] and a diffusive dynamics [5]. Our main result here is that the situation is actually much more complicated for the KH model, leading to an essentially different structure of the phase diagram (Fig. 4) and to a coexistence of different types of spectra in the various regions. If we fix L and vary K we indeed at first observe dynamical localization, but as K increases a transition to unbounded spreading takes place, characterized by some nonzero exponent α: $\langle\Delta n_t^2\rangle\sim t^{\alpha}$. For each sufficiently high L we indeed observed such a transition at $K=K^*(L)<L$: The main feature of the phase diagram is thus a threshold for unbounded spreading which lies (for L big enough) in the

Harper subcritical (localized) region (we call this threshold the KH critical line). We add a few remarks: (i) Our investigation of parameter space is not so fine grained as to check whether the threshold is given by a smooth line. (ii) For very small L, K^* coincides with the critical value $K=L$. (iii) Our numerical work is confined to classically chaotic parameter pairs. We thus partition the $K<L$ region into two subregions: Regions I ($K<K^*$) characterized by dynamical localization, and region II ($K^*<K<L$), exhibiting unbounded spreading of the initial wave packet. The complementary region $K>L$ is in turn partitioned into regions I* and II*, dual (i.e., symmetric with respect to the line $K=L$) to I and II, respectively.

As regards the localized or delocalized nature of dynamics in the various regions we give numerical evidence based on three different indicators: (1) the long-time behavior of the wave function as characterized by the spreading $\langle \Delta n_t^2 \rangle$ and the related exponent α; (2) the long-time behavior of the integrated autocorrelation function (IAF) $C_{\rm int}(t)=t^{-1}\sum_{k=0}^{t}|\langle\psi_0|\mathbf{U}_{L,K}^{k}|\psi_0\rangle|^2$ (time-averaged probability of survival in the initial state); (3) a spectral analysis based on the reconstruction of the spectrum via a Cantor-set-like construction that we now briefly describe. At each step a covering is given by the band spectrum obtained by replacing $\hbar$ with some rational approximation. In particular a natural sequence of rational approximants $\{p_n/q_n\}$ is given by successive truncation of the continued-fraction expansions of the irrational parameter: By using well-known techniques [16], replacing $\hbar/2\pi$ with p_n/q_n leads, via the Bloch theorem, to a band spectrum, consisting of q_n bands whose length we denote by $l_{i(n)}$.

The application of the thermodynamic formalism (see [17]) to analyze the hierarchical presentation of the spectrum was pioneered by Kohmoto [18], and has been applied to investigate the critical line of the kicked Harper model in [15], to which we refer the reader for definitions and elementary properties of the thermodynamic functions considered [19]. In particular our interest will be focused on the scaling spectrum $s(\mu)$, which describes the distribution of band scaling factors $\{\mu\}$ ($\mu_{i(n)}=-\log l_{i(n)}/\log q_n$), defined by

$$\sum_{i=1}^{q_n} l_{i(n)}^{-\tau}=\int_{\mu_{\min}}^{\mu_{\max}} d\mu\, q_n^{s_n(\mu)+\mu\tau}, \quad s(\mu)=\lim_{n\to\infty} s_n(\mu).$$

In practice the convex envelope $S(\mu)$ of the scaling spectrum is obtained by a saddle-point evaluation of the integral and a Legendre transform: The detection of differences between the scaling spectrum and its convex envelope signals the appearance of phase transitions [20]. Extensive work on tight-binding Hamiltonians (reviewed in [21]) supports the view that the thermodynamic formalism represents a powerful tool to understand the nature of the limit spectrum: In particular, analysis of the Harper model leads to the following correspondence between $s(\mu)$ and spectral features: Absolute continuous spectrum leads to a single point [$s(\mu)=1$ for $\mu=1$, and denumerable Van Hove singularities contributing a vanishing $s(\mu)$ for $\mu=2$], singular continuous spectrum leads to a well-defined scaling spectrum whose support lies in the $\mu>1$ region, while in the case of the pure-point spectrum the limit which defines $s(\mu)$ does not exist, as bands shrink faster than exponentially.

We now report our results concerning the structure of the parameter space. The delocalized character of the dynamics above the KH critical line is supported by all the computed indicators. The spreading in momentum space persists over all integration time ($t_{\max}\sim 3\times 10^5$ kicks, employing a Fourier basis of 2^{17} unperturbed eigenstates to follow time evolution) above the critical line. The persistence of this spreading even when the IAF has apparently settled to a nonzero limit supports the view that this is not a transient phenomenon, due to unresolved point spectrum. A thermodynamic analysis of the spectrum along the previously sketched lines allows in

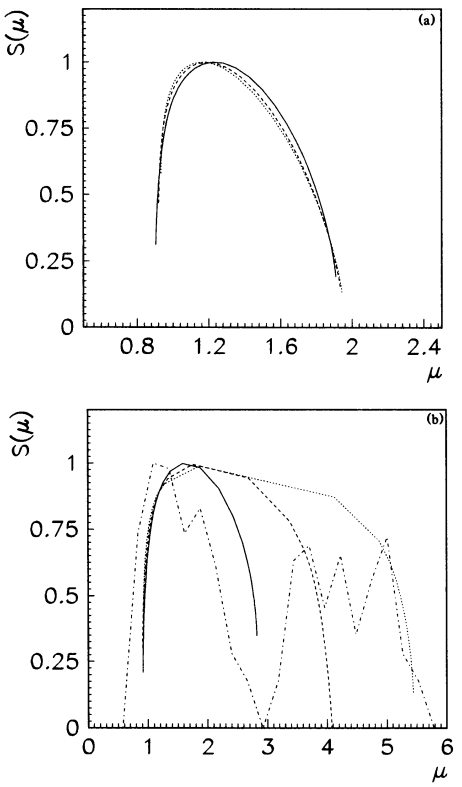

FIG. 1. (a) $S(\mu)$ for different rational approximants (solid line: 5/38; dashed line: 13/99; dotted line: 34/259) for $K=4$, $L=2$; notice the overall convergence to a limit curve. (b) $S(\mu)$ for different rational approximants (solid line: 5/38; dashed line: 13/99; dotted line: 34/259) for $K=4$, $L=7$: High-μ behavior exhibits nonconvergence (the dash-dotted line represents the scaling spectrum obtained by binning the μ scale and plotting a density histogram using bandwidths for $p_n/q_n=34/259$).

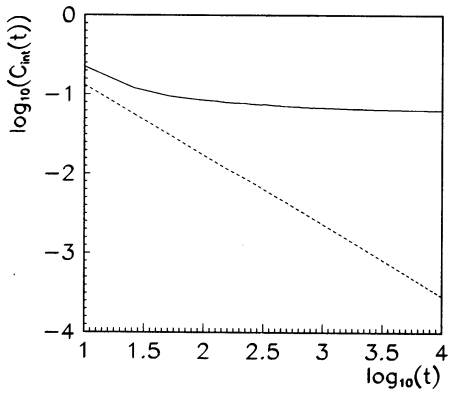

FIG. 2. Integrated autocorrelation function for $K=4$, $L=2$ (lower curve) (in the region dual to I), and for $K=4$, $L=7$ (upper curve) (region II).

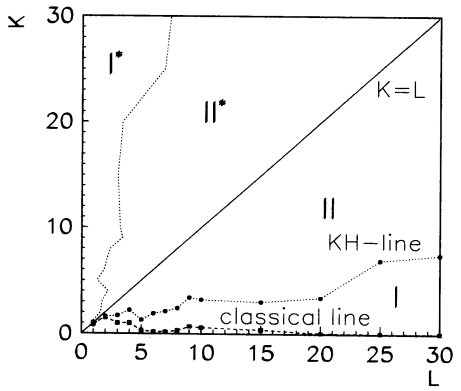

FIG. 4. Pictorial view of the phase diagram of kicked Harper model. We show the critical KH line and its symmetry around the $K=L$ line. We also added the classical chaotic border over which classical diffusion takes place (classical line).

many cases for a finer spectral resolution than obtainable via dynamical means, and yields results which agree with the phase diagram partition based on dynamical properties. More precisely in region I (localization) we do not observe any scaling feature, while region I* (dual conjugate to I) shows a well stabilized scaling spectrum (this indicates a purely continuous spectrum); see Fig. 1(a). Both region II and its dual II* display the coexistence of stable portions of $s(\mu)$ (left branch) with a high-μ tail not converging to a limit [see Fig. 1(b)]. We interpret these results as a strong indication of mixed spectrum, containing both pure-point and continuous components. This conjecture is confirmed by looking at the time dependence of the IAF, which in region I* steadily decreases over all inspected time and is therefore likely to tend to zero, while it approaches a finite limit (thus clearly indicating the presence of a pure-point component in the spectrum [22]) both in region II and for its image under duality (see Fig. 2). This phenomenology reflects the interchanging of continuous and pure-point components under a duality transformation of the parameters [8]. Figure 3 illustrates some typical behavior of the dynamical exponent α which was observed over the specified integration time: Notice how α decreases by passing through the critical line (the choice of K/L in the figure is not meant to indicate any simple scaling of the dynamical exponent). The appearance of values of α different from 1 (already signaled in [15] on the critical line) is another point of difference with the available data for the Harper model; at the same time, these regimes of anomalous diffusion definitely indicate that the long-time behavior of the quantum KH model is hardly related to the underlying classical dynamics. This fact, and the observation that region I extends well beyond the transition to chaotic diffusion for the classical mapping, lead to the intuition that the behavior of the KH model is not to be considered an exception to the phenomenon of quantum suppression of classical diffusion.

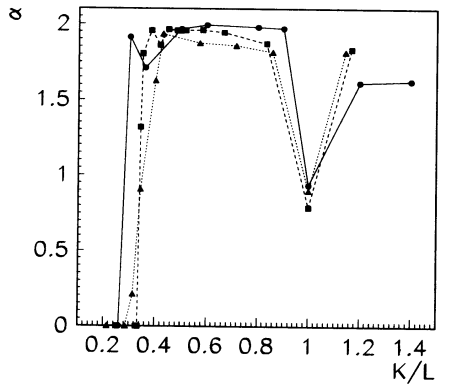

FIG. 3. Dynamical exponent α vs K/L for some fixed values of L. Circles are for $L=5$ and $1.3<K<7$, squares for $L=6$ and $1.5<K<7$, and triangles for $L=7$ and $1.5<K<8$. Notice the minimum corresponding to the critical line. Each α was determined by examining a time series up to 3×10^4 kicks.

We may thus conclude by illustrating the phase diagram of the kicked Harper model (see Fig. 4): Region I is characterized by dynamical localization and a pure-point spectrum; its dual conjugate I* exhibits unbounded spreading and a purely continuous spectrum. Both region II and its dual conjugate II* are characterized by unbounded spreading and coexistence of continuous and pure-point spectra (signaled by lack of convergence of the rightmost branch of the scaling spectrum and nonzero limit of the integrated autocorrelation function). In this region the observed values of the diffusion exponent and the thermodynamic analysis suggest the existence of a singular continuous component. Further analysis of the multifractal structure of the spectrum and of its relationship to the diffusion exponent is now in progress.

We acknowledge useful discussions with Dima Shepelyansky. We also would like to thank Alberto Cominelli for computer assistance.

[1] *Chaos and Quantum Physics,* edited by M.-J. Giannoni, A. Voros, and J. Zinn-Justin (North-Holland, Amsterdam, 1991).
[2] *Quantum Chaos—Theory and Experiment,* edited by P. Cvitanović, I. C. Percival, and A. Wirzba (Kluwer, Dordrecht, 1991).
[3] P. Leboeuf, J. Kurchan, M. Feingold, and D. P. Arovas, Phys. Rev. Lett. **65**, 3076 (1990).
[4] F. M. Izrailev, Phys. Rep. **196**, 299 (1990).
[5] T. Geisel, R. Ketzmerick, and G. Petschel, Phys. Rev. Lett. **66**, 1651 (1991).
[6] P. G. Harper, Proc. Phys. Soc. London A **68**, 874 (1955).
[7] R. Z. Sagdeev, D. A. Usikov, and G. M. Zaslavsky, *Nonlinear Physics* (Harwood, Chur, 1988).
[8] J. Bellissard and A. Barelli, in *Quantum Chaos—Theory and Experiment* (Ref. [2]).
[9] I. Guarneri and F. Borgonovi, J. Phys. A (to be published).
[10] R. Lima and D. Shepelyansky, Phys. Rev. Lett. **67**, 1377 (1991).
[11] T. Geisel, R. Ketzmerick, and G. Petschel, Phys. Rev. Lett. **67**, 3635 (1991).
[12] R. Ketzmerick, G. Petschel, and T. Geisel, Phys. Rev. Lett. **69**, 695 (1992).
[13] S. Aubry and G. André, Proc. Israel Phys. Soc. **3**, 133 (1979).
[14] D. Shepelyansky, in *Quantum Chaos—Theory and Experiment* (Ref. [2]).
[15] R. Artuso, G. Casati, and D. Shepelyansky, Phys. Rev. Lett. **68**, 3826 (1992).
[16] S.-J. Chang and K.-J. Shi, Phys. Rev. A **34**, 7 (1986).
[17] D. Ruelle, *Thermodynamic Formalism* (Addison-Wesley, Reading, 1978), see [15] for other relevant references.
[18] M. Kohmoto, Phys. Rev. Lett. **51**, 1198 (1983); C. Tang and M. Kohmoto, Phys. Rev. B **34**, 2041 (1986).
[19] Our choice of the thermodynamic formalism prevents a direct comparison between dynamical exponents and fractal indices like D_1 and D_2 [see I. Guarneri, Europhys. Lett. **10**, 95 (1989) and [12]]. This would be possible by taking into account the scaling properties of the spectral measure: Our choice, however, proved to be more reliable in controlling finite-order effects.
[20] R. Artuso, P. Cvitanović, and B. G. Kenny, Phys. Rev. A **39**, 268 (1989).
[21] H. Hiramoto and M. Kohmoto, Int. J. Mod. Phys. B **6**, 281 (1992).
[22] The limit value of the IAF tends to get smaller as K is increased by keeping L fixed: This indicates that the pure-point component of the spectral measure is likewise decreasing.